Available online at www.sciencedirect.com

ScienceDirect

Applied Surface Science 253 (2006) 2031–2037

applied surface science

www.elsevier.com/locate/apsusc

Studies on electrodeposition of Fe–W alloys for fuel cell applications

C.N. Tharamani [a], Parthasarathi Beera [b], V. Jayaram [b], Noor Shahina Begum [a], S.M. Mayanna [a,*]

[a] *Department of Post-Graduate Studies and Research in Chemistry, Central College, Bangalore University, Bangalore 560 001, India*
[b] *Solid State and Structural Chemistry Unit, Indian Institute of Science, Bangalore 560 012, India*

Received 21 March 2005; received in revised form 21 February 2006; accepted 28 March 2006
Available online 15 May 2006

Abstract

Electrodeposition of Fe–W alloy has been carried out from acidic triammonium citrate (TAC) complex bath solution. The deposit is characterised by XRD, SEM, EDAX, XPS and polarization techniques. The alloys are amorphous and become partially crystalline on heat treatment. The composition (Fe/W) of elements in the coating and their oxidation states vary from the surface to the bulk of the material. The coatings exhibit as novel electrode material with low over voltage and good corrosion resistance for anodic oxidation of methanol in H_2SO_4 medium. The anodic peak current, a measure of oxidation reaction rate is considerably high on Fe–W alloy when compared to pure Fe and also the relative surface area of Fe by alloying it with W found to increase by 1200-fold.

Keywords: Electrodeposition; Fe–W alloys; Surface analysis; Anode material; Fuel cell; Corrosion resistance

1. Introduction

Tungsten forms alloys with iron group metals [1] and retains functional properties (mechanical, magnetic, etc.) even at elevated temperature. Hence, these alloys find wide spread applications in industrial sector. It is difficult to electrodeposit these alloys from aqueous solution because of the co-deposition of hydrogen and tungsten is reluctant metal to deposit. Attempts have been made to coat these alloys by electroplating technique using tailor made plating bath solutions [2,3].

Methanol oxidative fuel cell is a prospective power source since it is an easily refuelable power stack in the electrically driven vehicles [4]. It is almost on the verge of abandonment because of the facts—methanol oxidation reaction is kinetically sluggish and oxidation reaction intermediates can seriously poison the anode materials [5]. Exhaustive literature is available on the development of new electrodes of which few reports are noteworthy. Composites of Pt [6,7] with Ru, WO_3^{2-} and Ni–Pd [8] alloys are used as anode in methanol oxidative fuel cell. However, the preparative procedures of these materials are tedious and are not economically viable.

Alloys of tungsten exhibit good corrosion resistance towards highly corrosive media [9] which is one of the pre-requisites of electrode materials to perform better in fuel cell electrolytes. As a part of wide spectrum of work in our laboratory in the development of new electrode materials for H_2–O_2 and methanol oxidative fuel cells [10–14], in this communication we report on the electrochemical synthesis and characterisation of Fe–W alloys to use as effective anode for methanol oxidation in H_2SO_4 medium. The electrode preparation is simple and cost effective. The prepared electrode is stable and acts as electrocatalyst during anodic oxidation of methanol.

2. Experimental

All solutions were prepared by using AR grade chemicals and distilled water. Fe–W alloys were deposited on copper foils (99.9%, 10 mm × 10 mm × 0.5 mm). Prior to deposition, copper foils were pre-treated by standard procedures [15]. Plating experiments were carried out in all glass three-necked-cell of 250 ml capacity at 303 K for 30 min to 1 h. The pH of the bath solution was maintained at 3.0 using dil. $NaOH/H_2SO_4$.

* Corresponding author. Tel.: +91 80 23301726; fax: +91 80 23219295.
E-mail address: smm_chem@yahoo.co.in (S.M. Mayanna).

0169-4332/$ – see front matter © 2006 Elsevier B.V. All rights reserved.
doi:10.1016/j.apsusc.2006.03.077

Both deposition of the alloys and polarization in H_2SO_4–methanol mixture were carried out under galvanostatic conditions (1–100 mA/cm^2) using a potentiostat/galvanostat (EG & G PAR 362). A large platinum foil and saturated calomel electrode were used as auxiliary and reference electrodes, respectively. A luggin capillary between working electrode and reference electrode was used to minimise the IR drop. The surface morphology and phases of deposited alloy were studied by scanning electron microscopy (SEM) and X-ray diffractometer (XRD) (Simen D5005 with Cu Kα radiation). Coatings of alloys were de-stripped in 1:4 nitric acid–water mixture, iron and tungsten contents in the alloy were estimated calorimetrically [16,17].

X-ray photoelectron spectroscopy (XPS) of the deposited thin films were recorded on an ESCA-3 Mark II spectrometer (VG Scientific Ltd., England) using Al Kα radiation (1486.6 eV). The binding energies were evaluated with respect to C (1s) peak at 285 eV with a precision of ±0.2 eV. The samples were placed into an ultra high vacuum (UHV) chamber at 10^{-9} Torr housing the analyzer. Prior to mounting, the samples were kept in the preparation chamber at ultra high vacuum (10^{-9} Torr) for 5 h in order to desorb any volatile species present on the surface. Intermittent sputtering was performed by using defocused Ar^+ ion beam at low voltage and current over an area of 0.8 mm × 2.4 mm.

Sputtering was carried out to remove successive layer of few angstroms and to know the composition of the material in the particular layer. The experimental data were curve fitted with Gaussian peaks after subtracting a linear background. For Gaussian peaks, slightly different full width at half maximum (FWHM) was used for different chemical states. The spin orbit splitting and the doublet intensities were fixed as given in the literature [18]. The concentrations of different chemical states were evaluated from the area of the respective Gaussian peaks.

3. Results and discussion

3.1. Deposition of Fe–W alloys

The complexing agent in the plating bath solution produces good quality coatings during electroplating [19]. Based on the co-ordination chemistry of Fe^{2+} and WO_4^{2-} in aqueous solution, a few complexing agents are screened for Fe^{2+} ions at pH 3.0 using UV–vis spectrophotometry. An aqueous solution containing Fe^{2+} ions with triammonium citrate (TAC) showed two bands one around 11,730 cm^{-1} and other at 14,260 cm^{-1}, characteristics of $^4T_{2g} \rightarrow {}^5E_g$ transitions corresponding to octahedral metal–ligand complex of high spin (d^6) Fe(II) system (Fig. 1). Under the same experimental conditions, WO_4^{2-} ions failed to form complex with TAC.

Electroplating of Fe–W alloys is carried out under different experimental conditions such as current density (cd), pH and temperature using a plating bath solution with known concentrations of Fe^{2+} and WO_4^{2-}. TAC was used as a complexing agent for Fe^{2+} ions. Boric acid and sodium chloride were used in the bath as buffering agent and conducting salt, respectively. Dimethyl sulfoxide (DMSO) in the plating bath

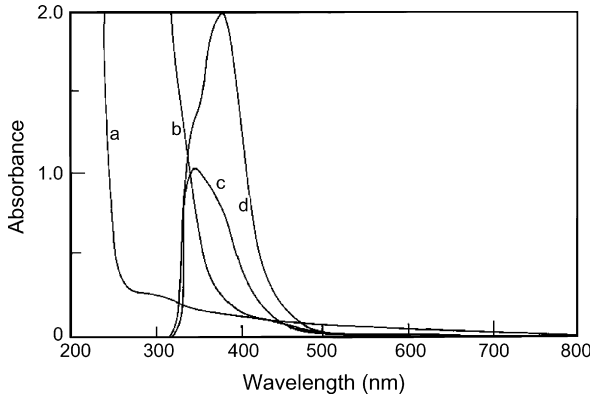

Fig. 1. UV absorption spectra of solutions: (a) TAC; (b) DMSO + Na_2WO_4; (c) FAS + TAC; (d) FAS + TAC + DMSO + Na_2WO_4.

solution improved the deposition rate. Based on the obtained results, the following bath composition and working conditions were fixed to get good quality alloy coatings. Composition: ferrous ammonium sulphate 0.1 M, Na_2WO_4 0.02–0.05 M, TAC 0.2 M, DMSO 0.05 M, H_3BO_3 30 g/l and NaCl 10 g/l; working condition: cd 10–100 mA/cm^2, pH 3.0, temperature-303 K, plating time-30–60 min, anode-stainless steel, cathode-copper foil.

3.2. Microstructure and surface morphology

Anodic oxidation of methanol is controlled by surface reaction [20] and comprehensive understanding of such a process needs good knowledge of microstructure and nature of the surface of anode material. In order to know some of these details, coatings obtained under different experimental conditions are taken for XRD, SEM and energy dispersive X-ray (EDAX) analysis.

XRD data of coatings on copper substrate without and with heat treatment are given in Table 1. The deposited alloy is

Table 1
XRD data of Fe–W alloy

As deposited			After heat treatment[a]		
Observed d (Å)	Std. ASTM[b] d (Å)	Phase	Observed d (Å)	Std. ASTM[b] d (Å)	Phase
2.102	2.120	Fe(1 0 0)	3.795	3.790	$Na_2W_4O_{13}$ (0 0 1)
				3.797	$Na_{0.02}WO_{2.8}$ (0 0 1)
2.066	2.062	W(2 1 1)	2.102	2.120	Fe(1 0 0)
				2.050	Fe_2W(2 0 0)
1.452	1.452	W(2 2 2)	2.033	2.027	Fe(1 1 0)
1.283	1.280	Fe_2W (0 0 6)	1.092	1.092	Fe_2W(2 1 5)
1.093	1.092	Fe_2W (2 1 5)	1.284	1.280	Fe_2W(0 0 6)
1.090	1.089	Fe_2W (3 1 2)			

Target: Cu kα; filter: Ni.
[a] 623 K under N_2 atmosphere for 5 h.
[b] 1999 JCPDS-International Centre for Diffraction Data, PCPDFWIN v. 1.30.

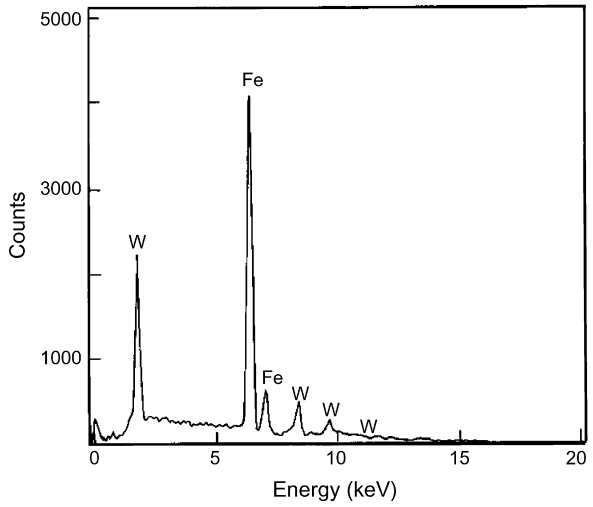

Fig. 2. Energy dispersive X-ray analysis of Fe–W alloy (as-prepared).

largely amorphous because the XRD patterns contain only broad and diffused bands with few low intensity peaks. However, on heat treatment, the coatings become crystalline with the formation of new phases. From the XRD patterns of the heat-treated sample, the particle size was calculated and found to be 350 Å. Fig. 2 gives the EDAX patterns of Fe–W alloy. The peak with respect to copper was absent. These results indicate that Fe–W coating is coherent and free from pores.

Fig. 3a shows a micrograph of as-prepared Fe–W alloy. The surface has the characteristics of a dense uniform coating with a nearly uniform grain size. The appearance of few black spots on the surface may be due to weakly adsorbed contaminants

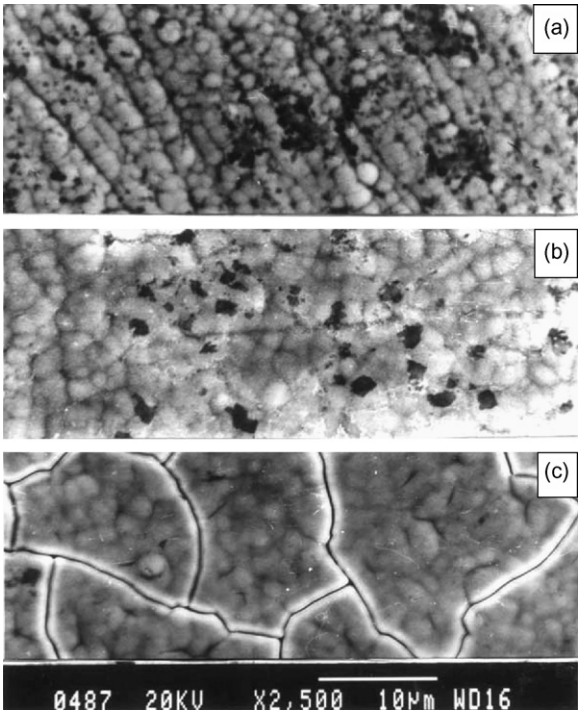

Fig. 3. Scanning electron microphotographs of Fe–W alloy: (a) as-prepared; (b) after polarized; (c) after heat-treated (623 K for 5 h under N_2 atmosphere).

derived from the slow electrolysis of organic components (TAC/DMSO). The surface is associated with less number of black spots after polarization of the coating in methanol–sulphuric acid mixture (Fig. 3b). Cracks are developed on the surface without black spots on heat treatment (Fig. 3c). The grain size of the heat-treated coating is evaluated from SEM data and found to be 355 Å which is comparable with the value obtained from X-ray data.

3.3. X-ray photoelectron spectroscopic studies

XPS studies of solid material give very useful information on the elemental composition and their oxidation states both on the surface and in the bulk of the sample (up to few layers).

In Fig. 4 XPS of Fe(2p) core level of plated Fe–W sample and the same after 5 and 15 min sputtering are shown.

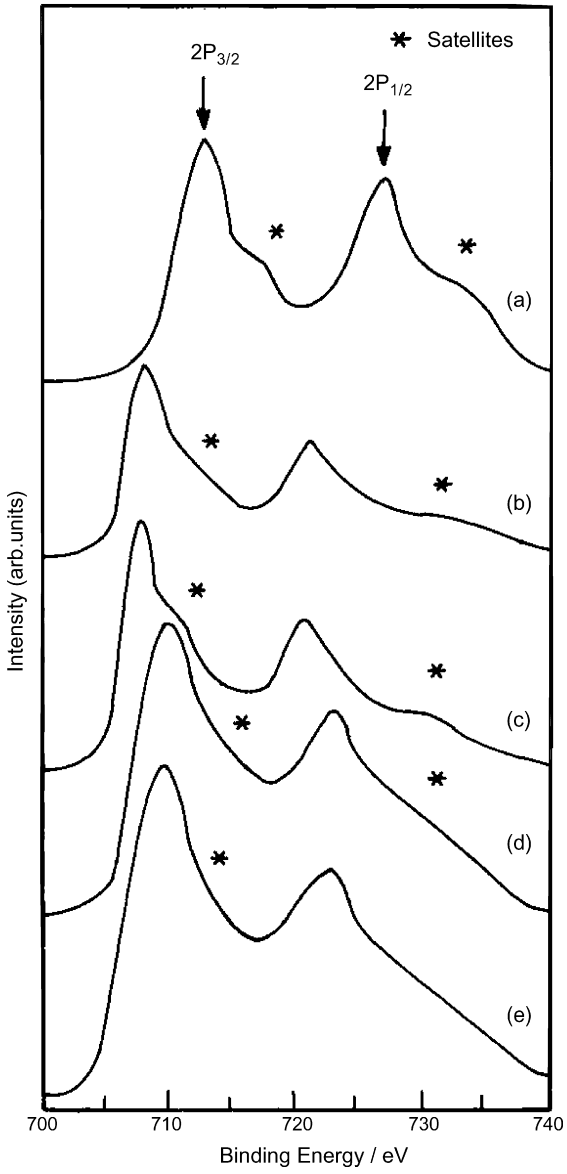

Fig. 4. XPS of Fe(2p) core level region of Fe–W alloy film: (a) as-prepared; (b)after 5 min sputtering; (c) after 15 min sputtering; (d) 5 min sputtering (heat treated); (e) 15 min sputtering (heat treated).

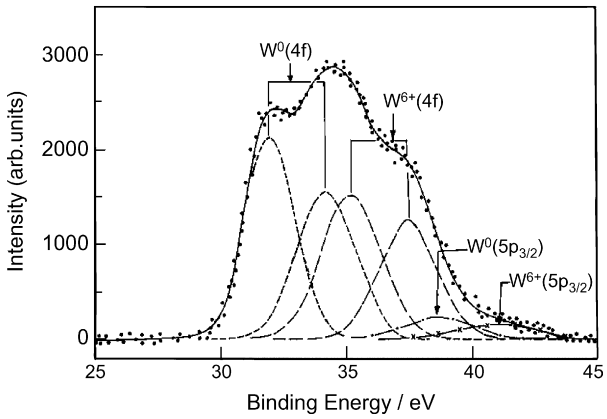

Fig. 5. XPS of W(4f) and W($5_{p3/2}$) core level regions of Fe–W alloy film after 5 min sputtering.

These results showed that Fe is in +3 oxidation state along with satellite peaks. Fe($2p_{3/2,1/2}$) peaks at 711.7 and 725.6 eV (Fig. 4a) are assigned to Fe^{3+} oxidation sate [21]. But the alloy film after 5 and 15 min sputtering shows the Fe($2p_{3/2,1/2}$) peaks at 704.4 and 720.5 eV which are characteristic of Fe metal (Fig. 4b and c). However, XPS data without sputtering do not vary with heat treatment. In contrast, Fe(2p) spectra of the heat-treated film after 5 and 15 min sputtering, consists of Fe($2p_{3/2}$) peaks at 710.1 and 710.0 eV, respectively. These data indicate the presence of Fe^{2+} in the sputtered film after heat treatment (Fig. 4d and e).

XPS of W(4f) core level region in as-prepared film shows peaks at 35.6 and 37.8 eV corresponding to W^{6+}($4f_{7/2,5/2}$). But the characteristics of the peak changes on sputtering for 5 and 15 min. Typical W(4f) and W($5p_{3/2}$) core level regions are shown in Fig. 5. The spectrum could be deconvoluted into two sets of spin–orbit doublets. Accordingly, W($4f_{7/2,5/2}$) peaks at 32.0, 34.2 and 35.2, 37.5 eV can be attributed to W^0 and W^{6+} oxidation states, respectively [22]. The less intense peaks at 38.7 and 41.0 eV are assigned to W^0($5p_{3/2}$) and W^{6+}($5p_{3/2}$), respectively. Similarly, W($4f_{7/2,5/2}$) peaks observed at 35.5 and 37.8 eV after heat treatment of the film indicate the presence of W^{6+}, where as metallic W as well as W in +6 oxidation state are also seen in the same heat-treated film after sputtering. Binding energies and relative intensities of different W species of as-prepared and heat-treated Fe–W films obtained under different conditions are given in Table 2.

Table 2
Binding energies and relative intensities of different W species as observed from W(4f) spectra of Fe–W film at different conditions

Sample	Species	Binding energy (eV) ($4f_{3/2}$)	Relative intensity (%)
Without sputtering	W^{6+}	35.6 (35.5)	100 (100)
5 min sputtering	W^0	32.0 (31.9)	58 (60)
	W^{6+}	35.2 (35.4)	42 (40)
15 min sputtering	W^0	32.0 (31.8)	61 (67)
	W^{6+}	35.3 (35.6)	39 (33)

Values with heat-treated samples (5 h, N_2 atmosphere at 623 K) are given in parenthesis.

Table 3
Surface concentration ratios of Fe(2p) to W(4f) in as-prepared Fe–W alloy film at different conditions

Sample	C_{Fe}/C_W
As-prepared	30
After 5 min sputtering	14
After 15 min sputtering	9

The surface concentration ratio of Fe(2p) to W(4f) is evaluated by the relation:

$$\frac{C_{Fe}}{C_W} = \frac{I_{Fe}\sigma_W\lambda_W D_E(W)}{I_W\sigma_{Fe}\lambda_{Fe}D_E(Fe)}$$

where C, I, σ, λ and D_E are the concentration, intensity, photo-ionization cross-section, mean escape depth and geometric factor, respectively. Integrated intensities of Fe(2p) and W(4f) peaks are accounted for calculating the concentrations. Photo-ionization cross-sections and mean escape depths are taken from the literatures [23,24]. The surface concentration ratios of Fe to W in as-prepared Fe–W alloy film obtained under different conditions are given in Table 3. The surface concentration ratio of Fe to W is 30 in as-prepared film suggesting the enrichment of Fe on the surface of Fe–W alloy film. But the Fe to W concentration ratio is found to decrease on successive sputtering. Similar trend is observed in the case of heat-treated sample.

3.4. Polarization studies

Alloys of Fe and W with sufficient thickness are prepared and used as electrode material (anode) for electrochemical oxidation of methanol in sulphuric acid medium since sulphuric acid is extensively used as electrolyte in methanol fuel cell [25]. Galvanostatic polarization curves for the methanol oxidation on Fe–W alloys are obtained at different current densities (10 and 100 mA/cm^2) in 1 M CH_3OH containing 0.5 M H_2SO_4 at 303 K

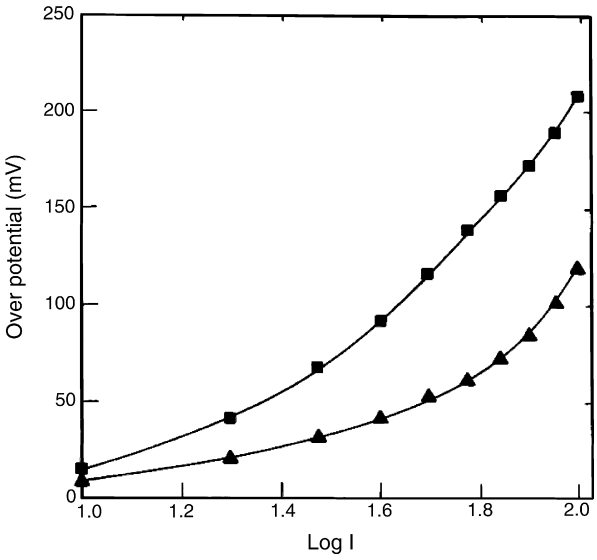

Fig. 6. Galvanostatic polarization diagrams for methanol (1 M) oxidation of in H_2SO_4 (0.5 M) medium on Fe–W alloy deposited at a current density of (■) 10 mA/cm^2; (▲) 100 mA/cm^2.

Table 4
Electrochemical parameters derived from polarization curves during methanol oxidation in H_2SO_4 on Fe–W (10% W) alloy at 303 K

Medium	Anodic tafel slope (mV/dec) (±5 mV)		i_{corr} (μA/cm^2)		η_{100} (mV) (±5 mV)	
	Electro deposit 1	Electro deposit 2	Electro deposit 1	Electro deposit 2	Electro deposit 1	Electro deposit 2
1 M CH_3OH + 0.5 M H_2SO_4	58	15	3.8	1.9	178	120 (105)[a]
1 M CH_3OH + 0.25 M H_2SO_4	75	25	0.85	1.5	140	100
0.5 M CH_3OH + 0.5 M H_2SO_4	112	48	0.35	0.96	200	152

Electrodeposit 1: obtained at cd 25 mA/cm^2. Electrodeposit 2: obtained at cd 100 mA/cm^2. The values on Fe–W electroplated at 100 mA/cm^2 are given in parenthesis.
[a] Heat treated at 623 K.

(Fig. 6). Low overpotential (measure of electrocatalytic activity) was observed in the case of alloy coating obtained at high current density. The electrochemical parameters for methanol oxidation on Fe–W alloy are given in Table 4. The overpotential depends on the concentrations of H_2SO_4 and methanol. A decrease in H_2SO_4 concentration or increase in the concentration of methanol results in the lowering of overpotential. Heat-treated Fe–W alloy is associated with low overpotential at low temperature, much lower than the value obtained with other electrode material [26] in a similar system.

Fig. 7 presents the cyclic voltammogram obtained on pure iron and Fe–W alloy deposit in 1 M CH_3OH containing 0.5 M H_2SO_4 at 50 mV/s. When polarized from −2000 mV on iron electrode, the zero current crossing potential (ZCCP) was found to be −510 mV followed by a small peak at −530 mV. On Fe–W alloy surface ZCCP was at −675 mV. Anodic peaks appeared at −575 mV followed by another peak at −500 mV. The peak at −575 mV is due to the oxidation of adsorbed hydrogen atoms. The catalytic activity was evaluated from the second anodic peak currents (Table 5).

The increase in catalytic activity upon heat treatment in the present system may be attributed to the change in nature of the surface of the deposit [27]. It is difficult to account the electrocatalytic activity of the electrode material because it is related to several complex parameters associated with surface and bulk properties of the coating: surface area, grain size and grain orientation, crystal structure, nature of chemical species and their composition, electronic conductivity, etc. In order to evaluate the relative increase in surface area of Fe–W by alloying W with iron, cyclic voltammetric experiments were carried out in the potential range −1500 to 0 mV at a suitable scan rate of 50 mV/s in a mixture of 1 M CH_3OH and 0.5 M H_2SO_4.

The electrocatalytic activity is related to increase in surface area as

$$\%\,\text{surface area increase} = \left(\frac{i_p(\text{Fe}-\text{W}) - i_p^0(\text{Fe}-\text{W})}{i_p^1(\text{Fe})}\right)$$

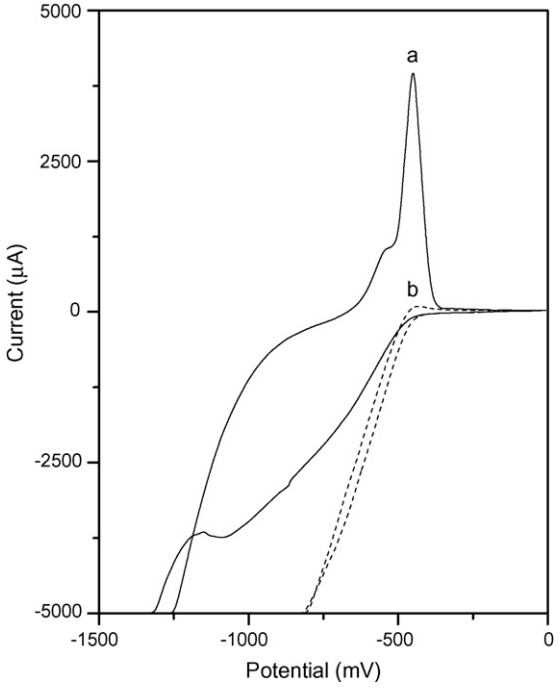

Fig. 7. Cyclic voltammograms obtained in 0.5 M H_2SO_4 and 1 M CH_3OH at a scan rate 50 mV/s and temperature 303 K: (a) Fe–W alloy; (b) Fe.

where i_p is the peak current due to CH_3OH oxidation and i_p^0 is the peak current due to H_2 oxidation, i_p^1 is the peak current due to CH_3OH oxidation on pure iron:

$$\%\,\text{surface area increase} = \left(\frac{4636 - 393}{3.6}\right) \times 100 = 1179\%$$

Pure iron is not a good electrode as it passivated due to the hydrolysis of the salt at pH > 5.

The alloys exhibited better corrosion resistance (Table 4) in H_2SO_4 medium. Prolonged electrolysis up to 100 h is conducted at 100 mA/cm^2 using alloys obtained at different current densities in 0.5 M H_2SO_4 containing 1 M methanol at 303 K. The anode is quite stable and exhibited steady

Table 5
Parameters derived from cyclic voltammogram in 1 M CH_3OH + 0.5 M H_2SO_4

Surface	ZCCP (mV) vs. SCE	First anodic peak		Second anodic peak	
		Potential (mV)	Current (μA)	Potential (mV)	Current (μA)
Pure iron	−510	–	–	−530	3.6
Fe–W alloy	−675	−575	393	−599	4636

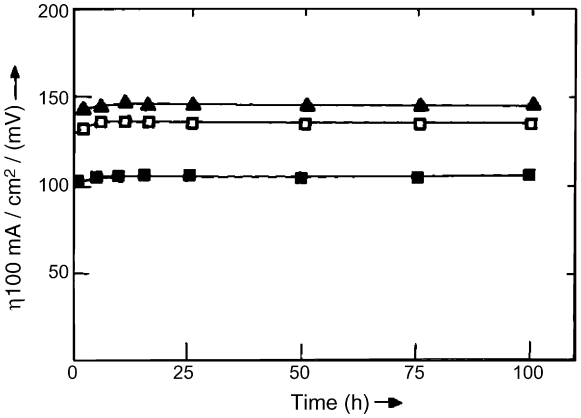

Fig. 8. Variation of over potential (η at 100 mA/cm^2) with time on coated alloys in 1 M CH_3OH and 0.5 M H_2SO_4 under different conditions: (▲) 50 mA/cm^2; (□) 100 mA/cm^2; (■) 100 mA/cm^2 (heat treatment).

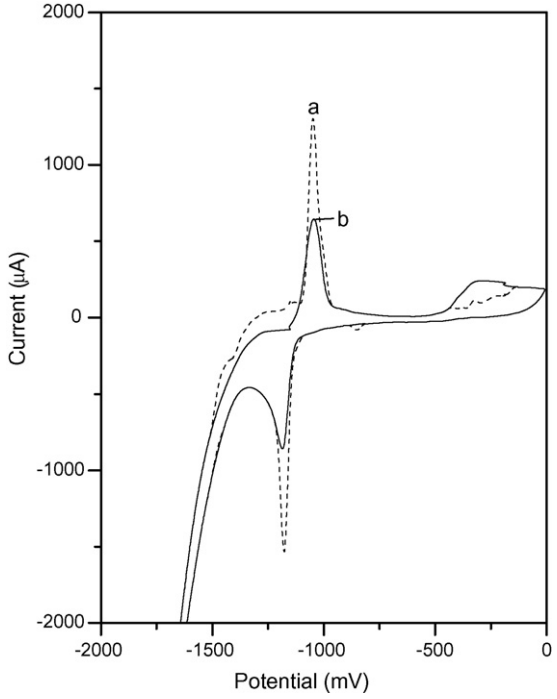

Fig. 9. Cyclic voltammograms obtained on Fe–W alloy at a scan rate 25 mV/s and temperature 303 K: (a) $ZnSO_4 + Na_2SO_4$ + formaldehyde; (b) oxidized mixture of methanol in H_2SO_4.

overpotential (±10 mV) (Fig. 8), which is one of the key characteristics of a high performing anode in a fuel cell.

The electro-oxidation of methanol is a complex process, which is retarded by the adsorption of reaction intermediates like CO, formaldehyde, etc., on the electrode surface [20]. In order to identity the reaction intermediate during oxidation cyclic voltammetric experiments are conducted. In aqueous solution under slightly acidic condition, zinc sulphate in presence of formaldehyde gives characteristic cyclic voltammogram [28]. In the present system, cyclic voltammogram is obtained on Fe–W alloy microelectrode using oxidised acidic (0.5 M H_2SO_4) methanol solution containing zinc sulphate. These results are compared with those obtained in acidic zinc sulphate solution containing formaldehyde. Similar results (Fig. 9) are obtained and confirm the presence of formaldehyde as intermediate during the oxidation of methanol in H_2SO_4 medium. A small portion of oxidised solution is coloured with chromotropic acid and UV absorption spectrum is taken. The absorption at 570 nm further confirms the presence of formaldehyde as reaction intermediate [20].

4. Conclusion

Electrodeposited Fe–W alloys from a plating bath solution with TAC as a complexing agent for Fe^{2+} ions, are partially crystalline. Oxidation states of Fe and W vary from the surface and to the bulk of the coating. Surface area of Fe gets enhanced by alloying it with W. The deposited alloys perform as a better anode material with low overvoltage for methanol oxidative fuel cell in H_2SO_4 medium at normal working temperature. The heat treatment of the coating improved the crystalline nature with the formation of new phases, corrosion resistance and electrocatalytic activity. Formaldehyde is a reaction intermediate which does not interfere during oxidation of methanol.

Acknowledgments

One of the authors (SMM) expresses his gratitude to the UGC, New Delhi for the financial assistance in the form of COSIST and to Dr. V.S. Muralidharan, CECRI, Karaikudi, Tamilnadu for helpful discussion.

References

[1] J.P. Wittewaur, T.G. Nietu, Adv. Mater. Process 142 (1992) 28.
[2] L. Ramesh, B.S. Sheshadri, S.M. Mayanna, Trans. IMF 76 (1998) 101.
[3] B.N. Maruthi, L. Ramesh, S.M. Mayanna, D. Landolt, Plat. Surf. Fin. 86 (3) (1999) 85.
[4] K. Kordesch, S. Simader, Fuel Cells and their Applications, VCH, Weinheim, 1996, p. 251.
[5] H. Matsui, Bull. Chem. Soc. Jpn. 60 (1987) 863.
[6] M. Watanabe, M. Uchida, S. Motoo, J. Electroanal. Chem. 229 (1987) 395.
[7] P.K. Shen, A.C.C. Tseung, J. Electrochem. Soc. 141 (1994) 3082.
[8] T. Shobha, C.L. Aravinda, P. Beera, S.M. Mayanna, Mater. Chem. Phys. 9868 (2003) 1.
[9] J. Bhattarai, E. Akiyama, H. Habazaki, A. Kawashima, K. Asami, K. Hashimoto, Corros. Sci. 40 (1998) 155.
[10] L. Ramesh, B.S. Sheshadri, S.M. Mayanna, in: Proceedings of the European Workshop on Chemistry Energy and Environment, Lisbon, Portugal, July 1997, R. Soc. Chem. 217 1998 505 (Special Publ. on Chem. Energy and Environment).
[11] L. Ramesh, B.S. Sheshadri, S.M. Mayanna, Int. J. Energy Res. 23 (1999) 919.
[12] T. Shobha, S.M. Mayanna, C.A.C. Sequeria, J. Power Sources 108 (2002) 261.
[13] T. Shobha, C.L. Aravinda, L. Gowmathi Devi, S.M. Mayanna, J. Solid State Electrochem. 7 (2003) 451.
[14] F. Shafia Hoor, M.F. Ahmed, S.M. Mayanna, J. Solid State Electrochem. 8 (2004) 572.
[15] R. Greef, R. Peat, L.M. Peter, D. Pletcher, J. Robinson, Industrial Methods in Electrochemistry, Ellis Horwood, Chichester, 1985, p. 355.
[16] G.D. Christian, Analytical Chemistry, 5th ed., John Wiley & Sons, Inc., New York, 2001, p. 723.
[17] X. Li, Y. Guo, S. Yao, J. Guo, Xuebai S S.D., Ziran Kexueban 22 (3) (1999) 255.

[18] D. Briggs, M.P. Seah, Practical Surface Analysis by Auger and X-ray Photoelectron Spectroscopy, Wiley, New York, 1984, p. 503.
[19] G. Salvago, P.L. Caralotti, Plating 59 (1972) 665.
[20] H. Matsui, A. Kunugi, J. Electro. Anal. Chem. 292 (1990) 103.
[21] A.M. Visco, F. Neri, G. Neri, A. Donato, C. Milone, S. Galvagno, Phys. Chem. Chem. Phys. 1 (1999) 2869.
[22] J. Haber, J. Stoch, L. Ungier, J. Solid State Chem. 19 (1976) 113.
[23] J.H. Scofield, J. Electr. Spectrosc. Relat. Phenom. 8 (1976) 129.
[24] D.R. Penn, J. Electr. Spectrosc. Relat. Phenom. 9 (1976) 29.
[25] A. Hamnett, P. Stevens, G.I. Troughton, Catal. Today 7 (1990) 219.
[26] He. Chunzhi, H.R. Kunz, J.M. Fenton, J. Electrochem. Soc. 144 (1997) 970.
[27] U. Adman, M.P. Dariel, E. Grunbaun, J.C. Lodder, J. Appl. Phys. 62 (1987) 1943.
[28] S. Shabana Begum, V.S. Muralidharan, S.M. Mayanna, Portug. Electrochim. Acta 19 (2001) 121.